Journal of Environmental Chemical Engineering 13 (2025) 118559

Contents lists available at ScienceDirect

Journal of Environmental Chemical Engineering

journal homepage: www.elsevier.com/locate/jece

Sustainable biowaste conversion into microporous carbons for efficient energy storage solutions in sodium-ion batteries

Meltem Yanilmaz [a,b,*], Busra Temel [b], Edip Bayram [c], Murat Tosun [d,**], Ismail Topcu [e], Juran Kim [f,**]

[a] Department of Textile Engineering, Istanbul Technical University, Istanbul, Turkiye
[b] Nanoscience and Nanoengineering, Istanbul Technical University, Istanbul, Turkiye
[c] Chemistry Department, Akdeniz University, Antalya, Turkey
[d] Department of Mechanical Engineering, Istanbul Technical University, Istanbul, Turkey
[e] Metallurgical and Material Science Engineering Department, Alanya Alaaddin Keykubat University, Antalya, Turkey
[f] Advanced Textile R&D Department, Korea Institute of Industrial Technology (KITECH), Ansan 15588, Republic of Korea

ARTICLE INFO

Keywords:
Microporous carbon
Cotton
Bio waste
Batteries

ABSTRACT

Sodium-ion batteries (SIBs) are prospective candidates for renewable energy storage technologies. However, SIB systems are still emerging, creating a demand for innovative, practical, and affordable active materials. Biomass-based hard carbons are promising anode materials for SIBs due to their easy accessibility, sustainability, and low cost.This study offers a novel, simple, and cost-effective method to produce microporous carbons from waste cotton using hydrothermal carbonization (HTC), KOH activation, and pyrolysis. Unlike previous studies on cotton-based carbons, the waste cotton-based microporous carbons were synthesized by the combination of HTC and KOH activation for the first time to be utilized as an anode in SIBs. Moreover, the influence of varying KOH concentrations on the structural and electrochemical properties of carbons was examined. The microporous carbon with a carbon/KOH ratio of 1/3, MC3, displayed a large surface area of 808 m^2/g, abundant microporosity, and achieved a high reversible capacity of 330 mAh/g at 0.1 A/g, and good cyclability with a reversible capacity of 280 mAh/g at 1 A/g after 400 cycles. These results demonstrated that the microporous structure of MC3 provides fast and efficient ion transfer and an increased contact area between the electrode and electrolyte. In addition, the integration of hydrothermal carbonization and KOH activation improves electrochemical performance and offers substantial economic benefits, while incorporating wastewater treatment and KOH recovery strategies into the process can enhance scalability and environmental sustainability for industrial-scale production. Therefore, this research presents a cost-effective and scalable approach using a sustainable source to produce microporous carbon anode materials for SIBs, significantly benefiting the energy sector.

1. Introduction

Sodium-ion batteries (SIBs) have been accounted as prospective candidates for high-capacity energy storage systems owing to the vast amount of sodium resources and low cost to meet the increasing worldwide demand for renewable energy technologies and to overcome environmental problems such as carbon emission and global warming caused by fossil fuels. Another reason for the emergence of SIBs is the limited availability of lithium-ion batteries (LIBs). However, Na-ions have a larger radius than Li-ions, which yields slower diffusion rates and a more severe impact on the electrode's structure, resulting in reduced capacity and unstable cycling performance. Therefore, to overcome these challenges, selecting ideal anode materials is critical for improving the performance of SIBs [1,2].

Recently, biomass-based carbon materials have drawn significant interest due to their abundance and sustainability. Due to their widespread availability, diverse biomass-based carbon materials, such as cellulose nanocrystals, cellulose, chitin, sugarcane bagasse waste, and onion peel, have been studied as anodes for SIBs [3]. Cellulose is one of the most widely used biopolymers to produce biomass-based carbon materials as anodes in SIBs due to its high abundance and biodegradability [1]. Apart from pristine cellulose, cotton, which includes a high

* Corresponding author at: Department of Textile Engineering, Istanbul Technical University, Istanbul, Turkiye.
** Corresponding authors.
E-mail addresses: yanilmaz@itu.edu.tr (M. Yanilmaz), tosunmur@itu.edu.tr (M. Tosun), jkim0106@kitech.re.kr (J. Kim).

https://doi.org/10.1016/j.jece.2025.118559
Received 11 May 2025; Received in revised form 11 July 2025; Accepted 7 August 2025
Available online 8 August 2025

amount of cellulose fibers, is a crucial element of the textile industry, and millions of tons of textile waste are either burned, causing air pollution, or sent to landfills, making it the second-largest landfill pollutant after plastics. Therefore, waste cotton can be a great alternative as a carbon precursor to produce anodes for SIBs [4]. Hard carbon, retaining the natural structure of the biomass precursor, can be readily produced through a straightforward pyrolysis process [5]. However, further modifications of their morphology and porous structure are needed to improve the electrochemical performance of hard carbon electrodes. For this reason, innovative methods such as hydrothermal treatment and chemical activation are being studied along with pyrolysis. Until now, there has been limited research about cotton-based hard carbon anodes for SIBs, including cotton-based hard carbon microtubes [6] showing a surface area of 38 m^2/g produced by direct carbonization at 1300 °C, and cotton-based hard carbon [7] with a surface area ranging from 1.6 to 285 m^2/g depending on the temperature. Waste-based cotton with a high surface area and excellent electrochemical performance has not been reported yet.

Hydrothermal carbonization (HTC) is a simple, green, and cost-efficient process that occurs in a low-temperature environment and water. Moreover, large-scale applications of HTC are developing and substantial challenges, including feedstock pretreatment, water management, and reactor design complexity have been addressed. Feedstock pretreatment is necessary for stable transfer and continuous feeding into reactors, while water management is required to remove by-products and pollutants from the process. Innovative reactor design is needed to enhance production efficiency and scalability. Upscaling HTC plants also demands the optimization of process parameters (temperature, pressure, residence time), and proper selection of reactor systems (batch or continuous). Companies such as CarboRem, TerrNova, and C-Green have established large-scale HTC plants and continue to generate innovative reactor designs and integrated treatment strategies. HTC offers environmental and economic benefits by reducing biomass waste and producing valuable biochar as well [8]. Moreover, combining HTC and pyrolysis enhances carbon yield and improves the electrochemical properties [9]. In most cases, carbon substances acquired from biowastes need an activation step via chemicals like KOH, HNO_3, or H_3PO_4 before the pyrolysis to enhance carbon porosity and increase the surface area, making it suitable for battery applications. KOH activation is a low-cost and short-term process that provides the formation of micropores [10]. Microporous carbons, with pore sizes less than 2 nm, exhibit a high surface area that provides more active sites for the adsorption and desorption of electrolyte ions. Moreover, the microporous structure facilitates the interaction between electrode and electrolyte and mitigates the volume expansion during cycling. Thus, the microporous structure of anodes considerably improves the electrochemical performance of SIBs [11]. In addition, combining HTC with KOH activation improves porosity, surface area, and carbon yield compared to the direct KOH activation and pyrolysis method. Direct KOH activation of biomass leads to excessive degradation of the organic substrate, causing lower yields and porosity. Thus, using HTC before KOH activation offers a more appropriate precursor to produce activated carbon [12]. While KOH activation and pyrolysis are commonly used methods to synthesize porous carbons, the combination of these methods with HTC for cotton waste is underexplored.

In this study, we applied an energy-efficient process to produce hard carbon anodes from waste cotton for SIBs for the first time and achieved a high surface area. Waste cotton-based microporous carbons were synthesized by combining hydrothermal processes at low temperatures, KOH activation, and pyrolysis. Moreover, the effect of KOH concentration on the structural and electrochemical properties of carbons was investigated. The resulting carbons were denoted as MC0, MC1, MC2, and MC3, corresponding to microporous carbons with different KOH proportions. The electrochemical performance of the samples was compared using the cycling performance tests. Among all the carbons studied, MC3 exhibited the highest porosity, with a BET surface area of 808 m^2/g. The MC3 achieved a high reversible capacity of 330 mAh/g at 0.1 A/g and good cycling stability with a capacity retention of 280 mAh/g at 1 A/g after 400 cycles. The outstanding electrochemical performance of the MC3 anode in SIBs can be ascribed to the combined effects of its microporous structure with a large surface area and the large interlayer spacing between graphitic layers.

2. Experimental

Waste cotton-based microporous carbons were prepared using HTC, KOH activation, and pyrolysis. A certain amount of cotton waste was immersed into 30 mL distilled water in a 100 mL Teflon-lined stainless-steel autoclave, and the autoclave was firmly closed and heated up to 250 °C for 4 h. After allowing it to cool to room temperature, the hydrochar was filtrated and washed with distilled water, then dried at 80 °C for 12 h. The hydrochar was mixed with 10 mL KOH solutions with different mass proportions of 1/1, ½, and 1/3. Then, hydrochar/ KOH mixtures were dried at room temperature for 24 h. The KOH/hydrochar mixtures and the hydrochar without KOH were pyrolyzed at 800 °C with a heating rate of 2 °C min^{-1} in an inert atmosphere for 2 h. After carbonization, the obtained carbons were washed with distilled water, filtered, and dried at 80 °C. The resulting carbons were denoted as MC0, MC1, MC2, and MC3, corresponding to microporous carbons with different KOH proportions (Table 1). The hydrochar/KOH ratios of 1:1, 1:2, and 1:3 were selected based on a previous study by Elisadiki et al. [13], in which increasing KOH ratios used in palm bark biomass facilitated a notable increase in porosity and enhanced electrochemical performance.

Scanning electron microscopy (SEM, Zeiss Sigma 300) and transmission electron microscopy (TEM, Hitachi High-Tech HT7700) were performed to investigate the morphology of microporous carbons. The structure was characterized by X-ray diffraction (XRD, PANalytical Empyrean XRD) and Raman spectroscopy (WITec alpha300 R). BET surface areas of the microporous carbons were examined by BET Analyzer (Quantachrome Corporation, Autosorb-6). Each sample was tested at least three times.

As prepared waste cotton-based microporous carbons were used as anodes in SIBs. The anode was prepared by mixing the MCs and sodium alginate in water to form a slurry. The slurry was coated on the copper foil and then dried at 60 °C for 12 h. Then, the copper foil was punched into 12 mm diameter discs. The electrochemical performance was measured with CR2032-type coin cells. The coin cells were constructed in an argon-filled glove box (O_2 < 0.5 ppm). The counter/reference electrode was a sodium foil (Na foil, Sigma), the glass fiber film (Whatman GF/D) acted as a separator, and the electrolyte was the solution of 1 M $NaClO_4$ in ethylene carbonate (EC)/propylene carbonate (PC) (v/v: 1/1), and the anode prepared by using alginate binder. Galvanostatic measurements and CV were performed on the battery testing system (Neware, Hefa) with a potential range of 0.1–2.5 V (vs. Na/Na+).

3. Results and discussion

Cotton is a widely available natural fiber that contains a high cellulose content (94 wt%). Due to its high carbon content, carbon skeletons can be produced by pyrolyzing cotton fibers. This work develops a simple and cost-effective approach to producing microporous carbons

Table 1
Summary table of MCs synthesis conditions.

MCs	HTC (250 °C, 4 h)	KOH activation	KOH concentrations (mol/L)	Mass proportions of hydrochar/KOH
MC0	+	-	0	0
MC1	+	+	0.86	1/1
MC2	+	+	1.81	1/2
MC3	+	+	2.74	1/3

from cotton waste. Firstly, hydrochar, the carbon-rich solid, was obtained by HTC of waste cotton at 250 °C. Then, the hydrochar was activated by KOH and pyrolyzed at 800 °C, which is labeled as MCX, where X represents the mass ratio of KOH to the hydrochar. The KOH activation provides a large surface area with high porosity in the carbons, while the pyrolysis process plays a role in increasing the carbon content and eliminating inorganic contaminants in hydrochar. The method for preparing waste cotton-based microporous carbons is illustrated in Figs. 1 and 2.

Fig. 3 shows the low and high-magnification SEM images of synthesized MC0(a, e), MC1(b, f), MC2(c, g), and MC3(d, h), respectively. Small pores and particle structures are visible in the high-magnification image of MC0. The structure of MC0 indicates that the hydrothermal treatment of waste cotton successfully triggered reactions such as hydrolysis, dehydration, condensation, and polymerization in the organic components of the precursor, which in turn created porosity in the produced carbons. The first step during HTC is the hydrolysis of cellulose, which allows subsequent reactions such as dehydration and decarboxylation to reduce the H/C and O/C ratios. Decarboxylation enables the degradation of carboxyl-carbonyl groups and releases the resulting CO_2 and CO gases. Then, an emulsion polymerization-like mechanism takes place, and the fibrous structure of MC0 turns into a porous structured hydrochar with the formation of spherical microparticles [14,15]. The carbon-KOH interactions in the subsequent KOH activation process were enhanced by the structural alteration of the waste cotton after HTC. As shown in Fig. 1, MC1, MC2, and MC3 display highly microporous and three-dimensional (3D) interconnected structures consisting of smaller nanoparticles, which can be attributed to the etching effect of KOH on MCs at high temperatures [16]. Fig. 3(f, g, h) presents high-magnification images of MC1, MC2, and MC3. These images demonstrate that combining HTC, KOH activation, and pyrolysis yields more uniform and smaller particles than using only HTC and pyrolysis. The MCs acquire more porous morphology with the increased mass ratio of KOH used in the carbon activation. In the KOH activation mechanism, hydrochars are etched by KOH, forming K_2CO_3 and K_2O via redox reactions that release H_2, CO_2, and CO gases. The formation of gases and metallic K intercalation into the carbon framework expands carbon lattices and creates micropores [17]. This unique morphology optimizes the interaction between electrodes and electrolytes for effective charge transfer and supports Na-ion transport by decreasing the diffusion pathways. Nie et al. [16] produced biomass-based porous carbon (BPC) anodes for LIBs from camellia oleifera shell via HTC, KOH activation, and carbonization at 800 °C and KOH activation, followed by HTC, significantly enhanced the porosity of carbon materials. The produced BPC showed a high reversible capacity. The improved results of BPC were attributed to its 3D porous structure providing rapid ion transport and increased interactions between electrodes and electrolytes. Similarly, Sangpresert et al. [18] used spent coffee ground-derived activated carbons (A-SCG) produced by HTC, KOH activation, and carbonization at 800 °C as anode materials for LIBs. A-SCG anodes showed a large surface area and retained a high discharge capacity. The high electrochemical performance of A-SCG anodes was attributed to their high surface area and high porosity, which offer more active sites, fast ion transport, and lower diffusive resistance.

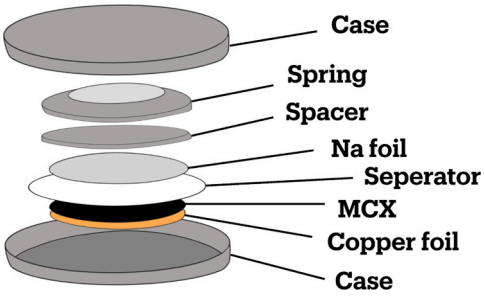

Fig. 1. Illustration of Na-ion cell architecture.

Fig. 4(a) shows the TEM image of MC3, highlighting its microporous structure—an advantage for the storage and transfer of Na ions [19,20]. Xu et al. [21] synthesized KOH-activated microporous carbons from pistachio nutshell as a supercapacitor material with highly interconnected nanosized pores. They obtained high electrochemical performance due to the cooperative effect of highly interconnected uniform micropores and high surface areas providing enhanced ion storage and fast ion transfer. The surface area and the pore structure of the waste cotton-based microporous carbons have been examined by N_2 adsorption-desorption tests. Fig. 4(b) discloses the N_2 adsorption-desorption isotherms of the waste cotton-based microporous carbons. All waste cotton-based microporous carbons show a type-I/IV isotherm exhibiting a distinct adsorption knee at low pressures and clearly defined plateaus, which demonstrates the existence of both mesopores and micropores in their structures [22]. Moreover, knee widening was observed at the low-pressure zone of MCs with increasing KOH ratio, denoting the broadening of micropores. In addition, the type H4 hysteresis loop seen in the isotherms of MC1, MC2, and MC3 also indicates the presence of mesopores [19]. It is observed that hysteresis loops become more apparent with increasing KOH ratio, indicating the expansion of micropores and formation of mesopores due to the stronger chemical etching [23]. The formation of micropores may result from the reduction of functional groups, the release of small volatile molecules, and the irregular contraction of the matrix [24]. As given in Table 2, the BET surface areas of MC0, MC1, MC2, and MC3 are 206, 624, 727, and 808 m^2/g, respectively, displaying an increasing tendency with increased KOH ratio. MC3 has the highest surface area among all samples, suggesting that combining HTC and KOH activation effectively regulates mesopores and micropores, significantly enhancing the specific surface area. This high surface area of MC3 could fasten ion transport, increase the electrode-electrolyte interactions, and thus improve the specific capacity of the anode [16]. Nandi et al. [25] produced rice husk-derived porous activated carbons for carbon capture via pyrolysis at 600 °C followed by KOH activation at 400 and 600 °C. They reported that the increasing KOH ratio led to a higher surface area, as more KOH was available to react with the carbon material, causing intense chemical reactions that developed micropores and pore enlargement during activation. Xiang et al. [26] fabricated an activated orange peel-derived hard carbon (OPDHC-A) as an anode for SIBs with microporous structure via direct KOH activation of orange peels followed by pyrolysis at 800 °C. They have found that the surface area increased from 357 m^2/g to 638 m^2/g with KOH activation. The obtained high electrochemical performance was assigned to the disordered activated microporous structure, which promoted electrolyte penetration and offered sites for storing Na-ions. Moreover, the microporous structure of carbons with a high specific surface area assisted rapid ion transfer and effective integration with active materials, which enhanced the electrochemical performance of the electrode [26,27].

Fig. 4(c–f) exhibits the pore size distributions of MCs. The porous structure of waste cotton-based microporous carbons comprised mesopores measuring around 2–30 nm and micropores with diameters smaller than 2 nm. Moreover, MC0 contains many mesopores with a large volume fraction of pores seen at around 30 nm. As seen in Table 2, a decrease in pore size and an increase in total pore volume were observed with higher KOH ratios, indicating an increase in micropores. MC3 shows abundant micropores with pore sizes below 2 nm. Furthermore, the increased KOH ratio not only provides the formation of micropores but also widens existing pores, leading to the development of mesopores through intense chemical reactions. The combined function of mesoporous and microporous structures will be advantageous in offering diffusion pathways for Na-ions and facilitating their storage during charge-discharge cycles [26,28]. However, high KOH concentrations can destabilize the carbon structure, causing pore shrinkage and framework expansion through severe etching [29,30]. Guo et al. [31]

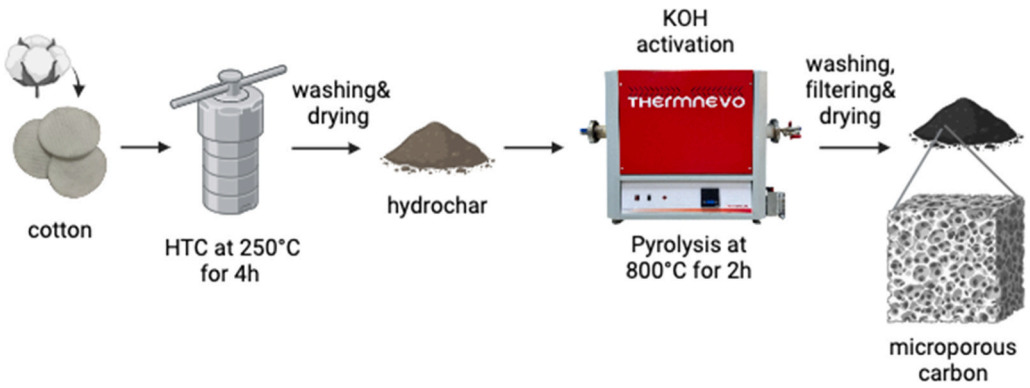

Fig. 2. A schematic representation of the MCX preparation process.

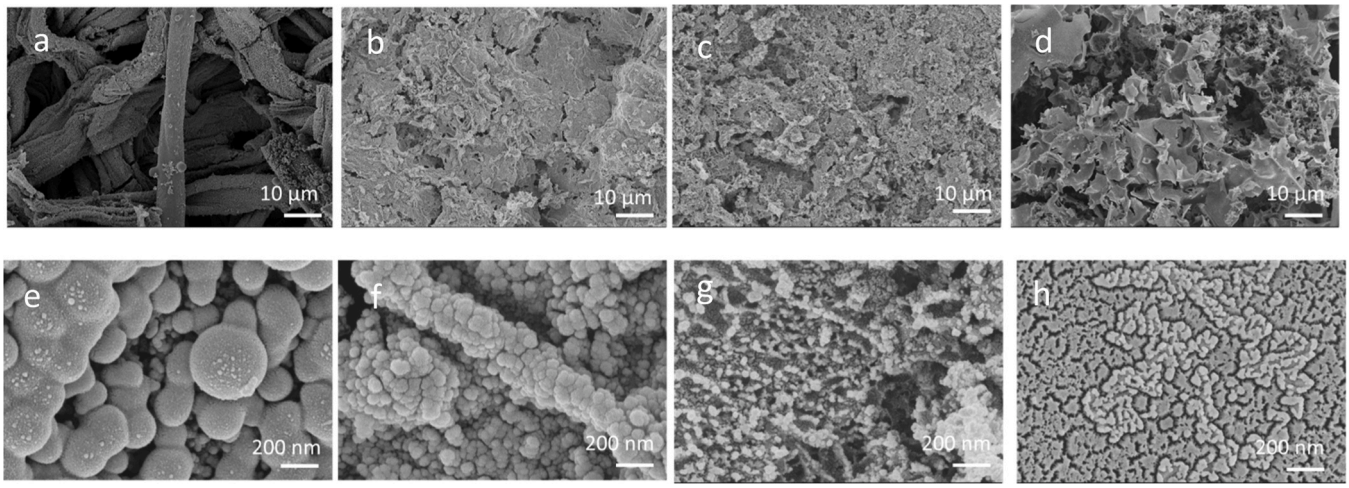

Fig. 3. SEM images of MCs after HTC and pyrolysis without KOH activation: MC0 (a, e), and with KOH activation: MC1(b, f), MC2(c, g), and MC3(d, h).

produced coal-derived microporous carbons using KOH activation with carbon: KOH ratios ranging from 1:1–1:5 and stated that when the KOH ratio was increased to 1:5, the specific surface area and total pore volume decreased, showing that the beyond a threshold, KOH activation leads to structural degradation and pore deformation.

Fig. 5 shows XRD patterns of MC0 (a), MC1(b), MC2 (c), and MC3 (d). All waste cotton-based microporous carbons showed distinct three diffraction peaks at $2\theta = 24°$, 43°, and 80°, corresponding to (002), (100), and (110) planes of disordered graphitic carbons, respectively, referring to amorphous carbon structure [32,33]. Furthermore, as shown in Fig. 5(a–d), with increasing KOH ratio, the (002) peaks exhibited low intensity and were slightly broadened, representing a more disordered structure of the samples after activation [32,34]. The interlayer spacing values of MCs calculated by Bragg's Law are approximately 0.42 nm, respectively, higher than the interlayer spacing of graphite (0.335 nm), facilitating the insertion of sodium ions into the graphitic layers. The increased interlayer spacing may be associated with the structural defects induced by KOH activation, and the high interlayer spacing in the waste cotton-based microporous carbons facilitates the insertion and extraction of Na-ions. The thickness of the graphitic domains (L) was estimated by the Scherer equation, utilizing the full width at half-maximum (FWHM) values of the (002) diffraction peaks. The thicknesses of the graphitic domains were calculated to be approximately 0.42, 0.40, 0.38, and 0.33 nm for MC0, MC1, MC2, and MC3, respectively. Arie et al. [35] produced activated porous carbons (APCs) from snake fruit peel as SIBs anode via pre-carbonization, followed by KOH activation at 800 °C. They reported a reduction in the thickness of graphitic domains from 0.87 to 0.79 nm as the KOH ratio increased from 1:1–1:3. This phenomenon is attributed to increased etching and penetration of the graphitic structure by KOH compounds during activation.

Fig. 6(a–d) shows that the Raman spectra of all waste cotton-based microporous carbons show G and D bands at 1356 and 1590 cm^{-1}, representing graphitic and disordered carbon, respectively. The intensity ratio between the D and G bands (ID/IG) indicates the level of carbon crystallinity and structural disorder. A lower ID/IG ratio signifies a higher degree of graphitization in the carbon material [28]. The intensity ratio of ID/IG for MC0, MC1, MC2, and MC3 was about 1.00, 1.01, 1.01, and 1.03, respectively. These ID/IG ratios were characteristic of porous carbon with a high level of structural disorder, supporting the results of the XRD analysis. Additionally, MC0, produced without KOH activation, exhibited a lower degree of disorder than the samples activated with KOH. Among these, MC3 possessed more defect sites, facilitating faster electron transfer and Na-ion insertion [36,37]. Wang et al. [36] synthesized peanut skin-derived hierarchical porous carbon as an anode for SIBs via HTC followed by KOH activation, and they observed higher specific capacity with increasing ID/IG ratio. They also reported that KOH activation tended to disrupt the graphitic regions within the carbon matrix, which accounted for the higher degree of disorder monitored in the samples prepared with higher quantities of KOH. Arie et al. [35] also assigned that the level of disorder in carbons increased in proportion to the mass ratio of KOH. Guo et al. [31] observed increased ID/IG values with increasing KOH ratios, indicating that more intensive KOH activation leads to the generation of defects and lots of micropores in the carbon matrix. Based on the results of SEM, TEM, N_2 adsorption-desorption isotherms, XRD patterns, and Raman spectra, the

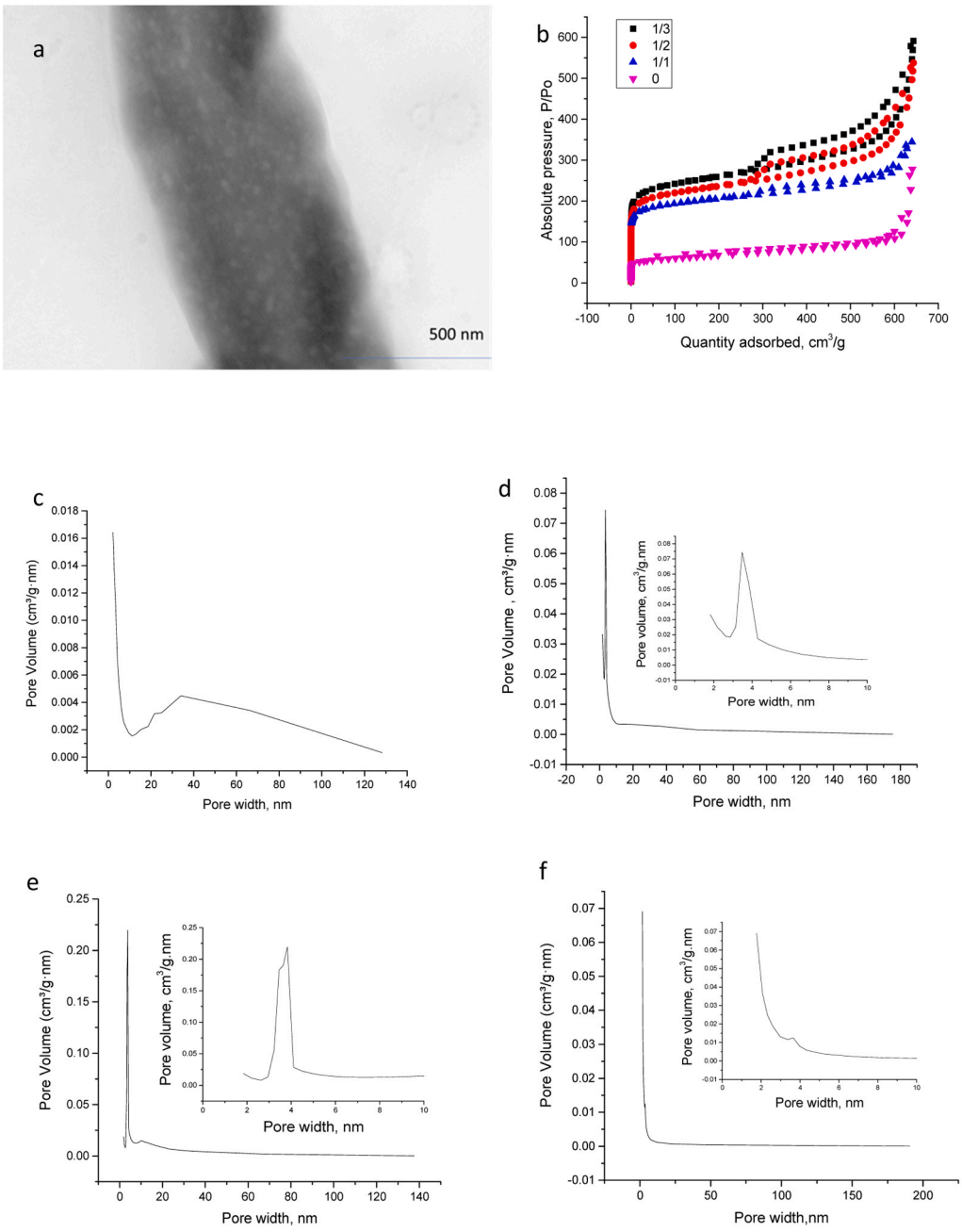

Fig. 4. TEM image of MC3(a), N_2 adsorption-desorption isotherms (b), pore size distributions for MCs after HTC and pyrolysis without KOH activation: MC0 (c), and with KOH activation: MC1 (d), MC2 (e), MC3 (f).

Table 2
Physical parameters for waste cotton-based microporous carbons.

	BET Surface Area, m^2/g	Pore size, nm	Total pore volume, V_{total} (cm^3/g)	V_{micro} (cm^3/g)
MC0	206	3.5	0.2	0.04
MC1	624	2.8	0.4	0.21
MC2	727	2.5	0.4	0.23
MC3	808	2	0.6	0.31

waste cotton-based microporous carbons produced through KOH activation exhibited a microporous structure that could enhance electrolyte penetration and offer sites for the storage of Na-ions [19,26].

The electrochemical performance of waste cotton-based microporous carbons as anodes was evaluated by half-cell configurations in coin-type cells. Fig. 8(a) shows the initial three CV curves of all waste cotton-based microporous carbons at a scan rate of 0.1 mV s^{-1} within a voltage range of 0.01–2.5 V. For MC3, the redox peak located below 0.2 V is due to the reversible insertion of Na-ions into MC3 and the adsorption of Na-ion on the porous surface [19]. The reduction peak at 1.2 V is observed in the first cycle and disappears in subsequent cycles, which is ascribed to the electrolyte decomposition and the SEI layer formation [38]. The oxidation peak at 0.5 V refers to the extraction of Na-ions [35]. The overlapped CV curves in subsequent cycles demonstrate the good cycling stability and reversible Na-ion storage. The galvanostatic charge−discharge (GCD) tests of all samples were carried out between 0.01 and 2.5 V at a current density of 0.1 A/g, as shown in Fig. 7. The first discharge-charge capacities of MC3, MC2, MC1, and MC0 are 480/380, 400/280, 300/200, and 250/130 mAh/g, respectively. Accordingly, the initial Coulombic efficiency (ICE) of MC3, MC2, MC1, and MC0 were

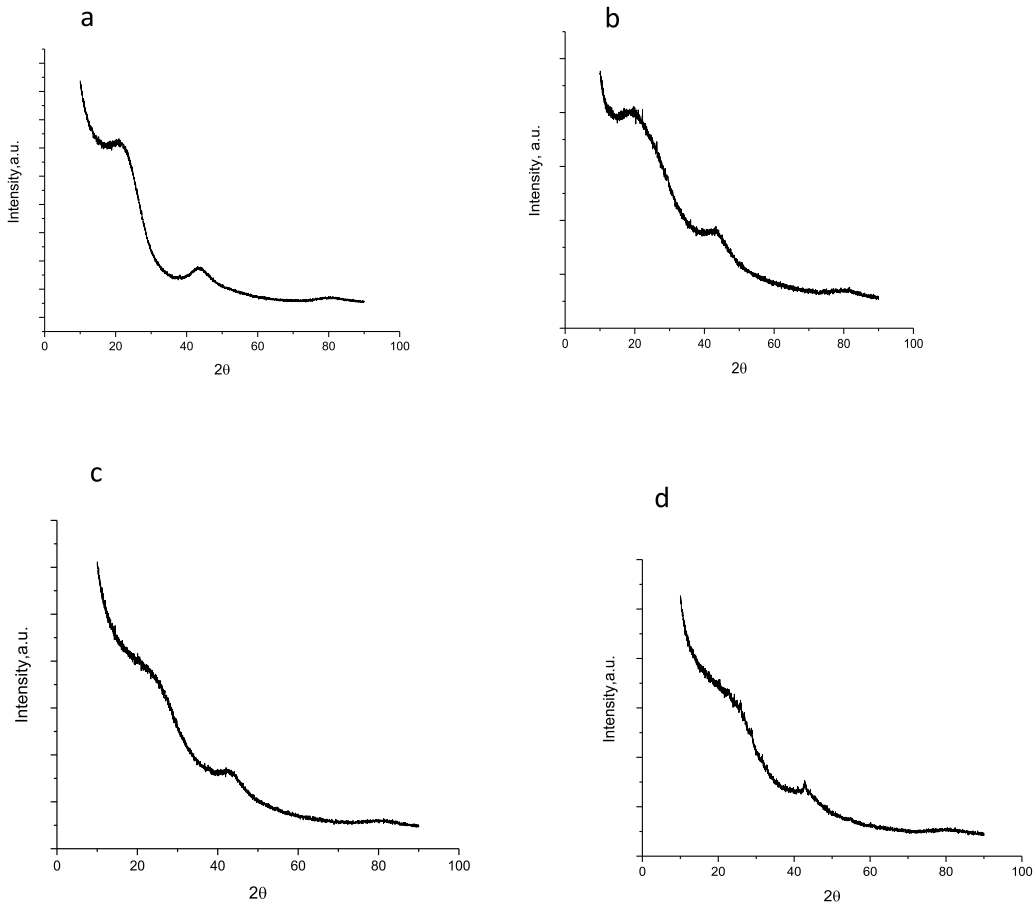

Fig. 5. XRD patterns of MCs after HTC and pyrolysis without KOH activation: MC0 (a), and with KOH activation: MC1(b), MC2 (c), and MC3 (d).

calculated to be 79 %, 70 %, 69 %, and 50 %. The profiles of all samples exhibited a sloped region ranging from 2.5 to around 0.15 V, primarily attributed to the adsorption of Na ions on the surface and at defect sites. They also showed a plateau region from around 0.15–0.01 V, typically linked to the slower filling of graphitic interlayers and pores [39]. It is observed that the ICE of waste cotton-based microporous carbons increases as the KOH ratio increases. The low ICE value is largely due to the SEI layer formation, irreversible adsorption of Na-ions, and side reactions [35]. Therefore, the high ICE value of MC3 reveals that activating waste cotton-based carbon with adequate KOH concentration can provide effective surface area, enabling enhanced Na-ion transfer and limited side reactions that improve electrochemical reversibility [19].

The GCD profile of hard carbons comprises two parts: the high voltage and the low voltage parts, which show the sloping and plateau regions, respectively. The sloping region is related to the intercalation of Na-ions into the disordered graphene layers, and the plateau region is assigned to the adsorption of Na-ions within the pores [40]. The voltage-dependent behavior of waste cotton-based microporous carbons can be more clearly elucidated by considering the Na-ion storage mechanism in hard carbons, as seen in Fig. 8. Today, the “house of cards” model was accepted as the standard model to disclose the basis of the sodiation mechanism. The model reveals the disordered graphitic structure of hard carbons, consisting of few-layered graphene structures within graphitic regions and micropores enclosed by graphitic structures [41]. The Na-ion storage mechanism of hard carbons mainly includes three stages: (1) adsorption on pore walls, (2) intercalation into the graphitic domains, and (3) formation of nanometer-size Na clusters in micropores. Unlike graphite, hard carbons consist of disordered graphene layers and have large interlayer distances, which makes them suitable for the intercalation of Na ions. Na ions can be incorporated between the graphitic layers in hard carbon and absorbed on the surface of the pores where the edges, defect sites, and functional groups are found. In addition, nanometer-sized Na clusters can form within the micropores of hard carbon, which contributes to the high capacity of the anodes [40,41].

Among all the waste cotton-based microporous carbons tested, MC3 demonstrated the highest sodium storage performance, achieving the highest initial discharge and charge capacities. This impressive electrochemical performance of MC3 was primarily due to the microporous disordered carbon structure and the wide interlayer spacing. The decrease in capacities from the first to the second cycle was attributed to the formation of the SEI layer, the side reactions with the electrolyte, and the irreversible entrapment of Na-ions within the active sites of the carbon structure. This initial capacity loss was frequent for carbon materials derived from biomass [42]. Moreover, combining HTC and KOH activation could adjust the surface properties of the carbons, which helped improve reversible Na-ion storage capacity. Wang et al. [36,43] synthesized microporous biomass-derived hard carbons as anodes from hemp bast fiber and peanut skin for SIBs via combining HTC and chemical activation processes. They reported high capacities of 163 mAh/g at 1 A/g over 2000 cycles and 148 mAh/g at 0.5 A/g after 200 cycles for hemp bast fiber-based and peanut skin-based carbons, respectively. These high capacities were ascribed to their morphologies with a large surface area, well-defined porosity, and increased lattice spacing between graphene layers.

Fig. 9(a) displays the cycling performance of MC0, MC1, MC2, and MC3 with reversible capacities of 100, 160, 230, and 330 mAh/g at a current rate of 0.1 A/g in 200 cycles, respectively. We can see that MC3, MC2, and MC1 have notably higher capacities than MC0. The KOH activation substantially improved the capacities of waste cotton-based

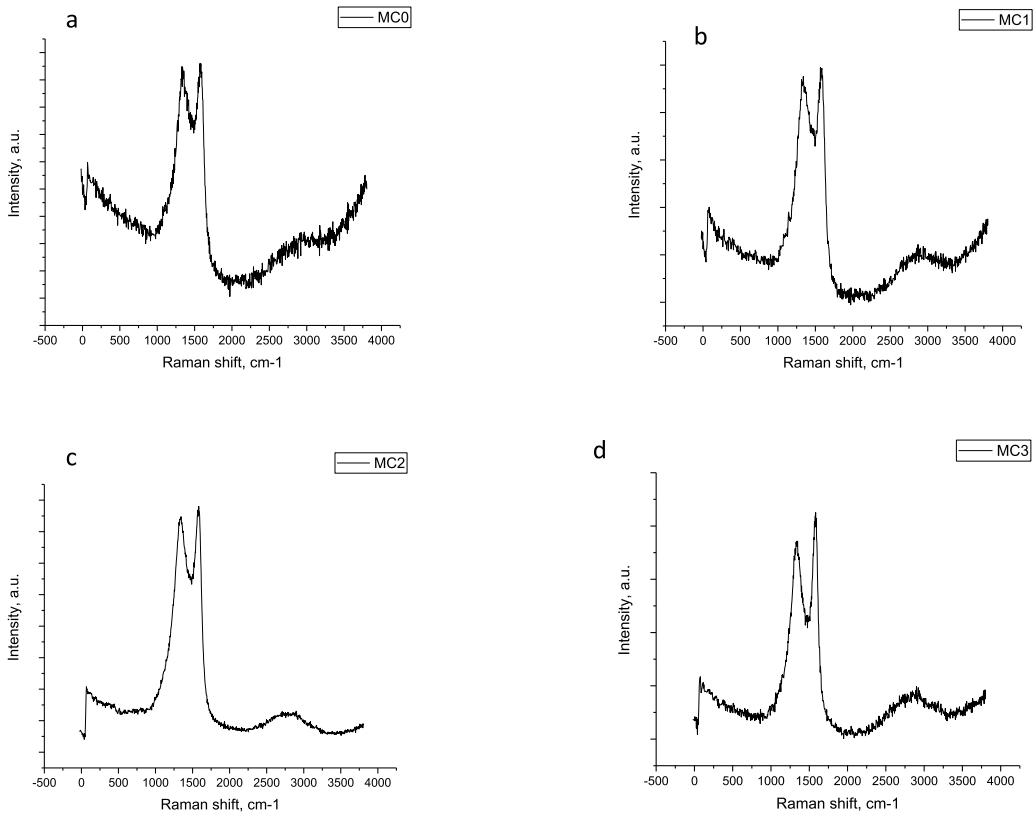

Fig. 6. Raman spectra of MCs after HTC and pyrolysis without KOH activation: MC0 (a), and with KOH activation: MC1(b), MC2 (c), and MC3 (d).

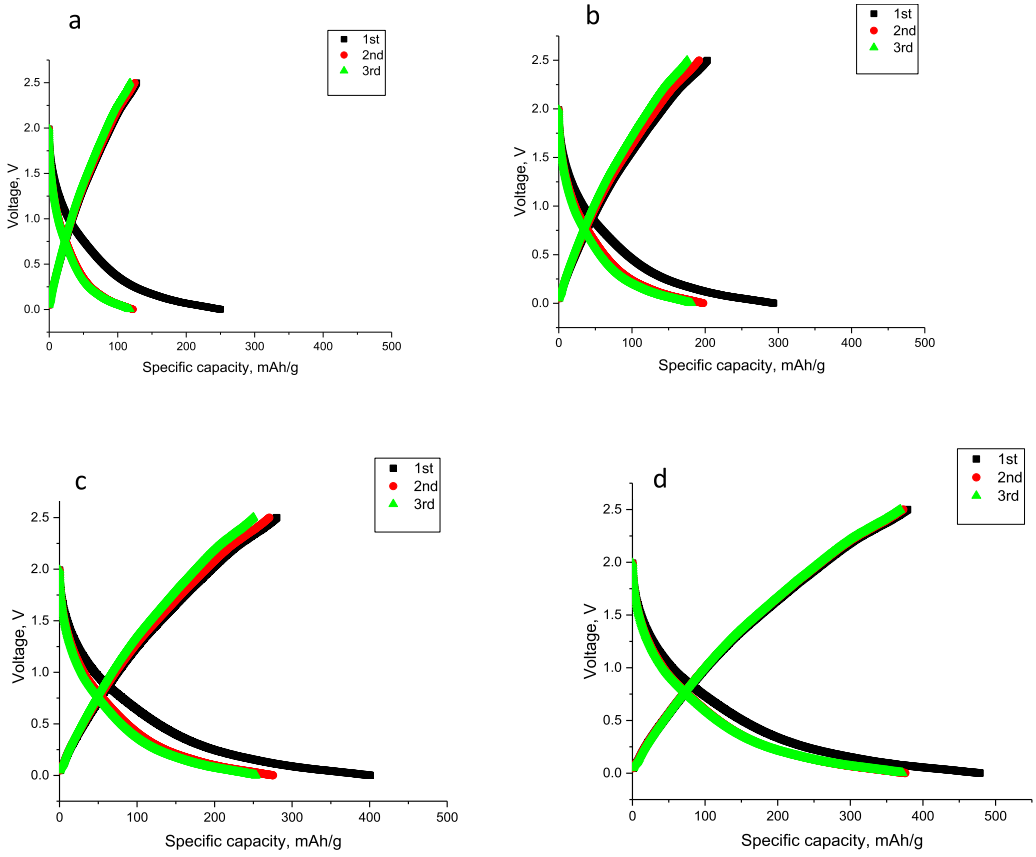

Fig. 7. First cycle discharge charge curves for MCs after HTC and pyrolysis without KOH activation: MC0 (a), and with KOH activation: MC1 (b), MC2 (c), and MC3 (d).

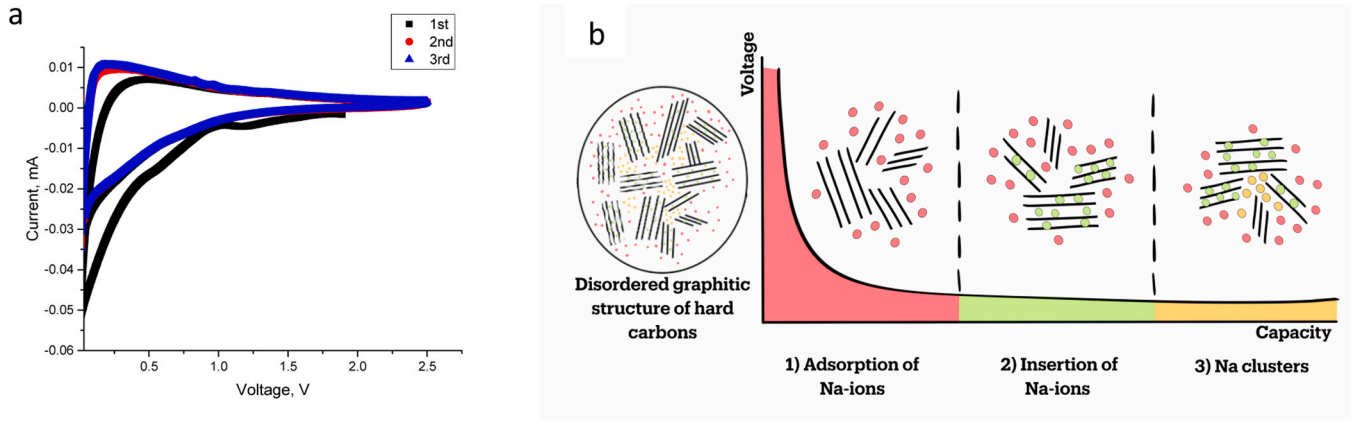

Fig. 8. CV curve for MC3 (a) and Schematic diagram of Na-ion storage mechanism in hard carbons, involving (1) intercalation of sodium ions into disordered graphene layers, (2) adsorption of sodium ions on pores and defects, and (3) clustering of sodium ions within micropores (b).

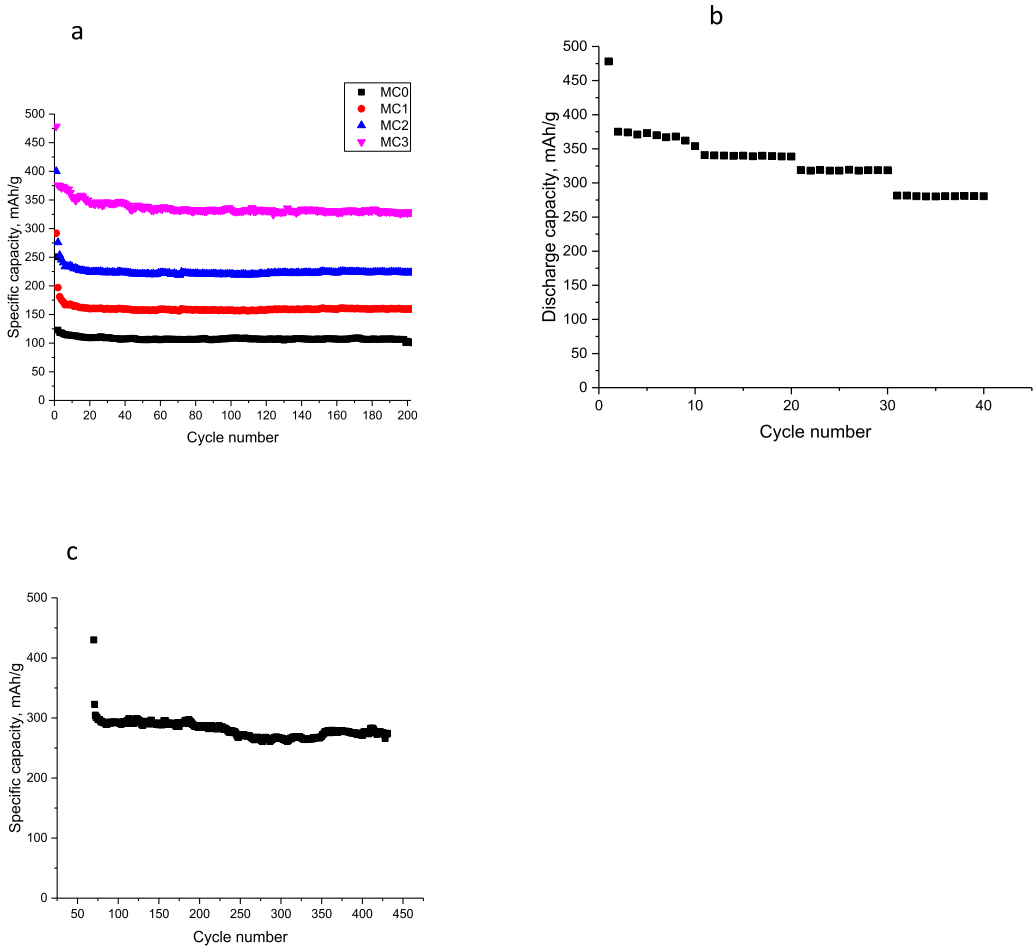

Fig. 9. Cycling performance of MCs after HTC and pyrolysis without KOH activation: MC0, and with KOH activation: MC1, MC2, and MC3 (a); rate performance (b) and high rate cycling performance (c) of MC3.

microporous carbons. MC3 showed the highest capacity due to its higher surface area, abundant micropores providing faster ion transport, enhanced contact area between electrode and electrolyte, and increased Na-ion storage. The capacity retentions were 40, 55, 58, and 69 % for MC0, MC1, MC2, and MC3, respectively. The capacity loss spotted during the first cycles could be associated with the insufficient stabilization of the SEI layer and the entrapment of Na-ions within the graphitic interlayers or at defect sites [36]. After initial cycles, all samples exhibited a stable cycling performance thanks to structural stability and a stable SEI layer formation. Zheng et al. [19] fabricated filter paper-derived hard carbon as anode for SIBs via pyrolysis and KOH activation and showed good cycling performance with a high reversible capacity of 286 mAh/g after 100 cycles at 20 mA/g. The outcome was assigned to its micro-nanostructure with a high surface area of 761 m^2/g. Its micro-nanostructure minimized the initial irreversible capacity loss by restricting the contact between the electrode and

electrolyte while boosting the capacity by promoting faster electron and Na-ion transfer through nanopores. Cao et al. [44] synthesized rape seed shuck-derived hard carbon anode for SIBs by HNO_3-assisted hydrothermal and pyrolysis processes, showing a surface area of 11.93 m^2/g with a capacity of 143 mAh/g at 100 mA/g after 200 cycles. This stable cycling performance was attributed to its sheet structure, which consists of nanoparticles and nanopores that facilitate fast Na-ion transfer. Antorán et al. [39] fabricated waste hemp-hurd-derived microporous carbons as anodes for SIBs via a three-step process: pyrolysis at 500 °C, K_2CO_3 activation with carbonization at 800 °C. They showed a specific surface area of 335.5 m^2/g and exhibited good cycling performance, with a capacity retention of 96 % at 2 A/g after 300 cycles. These results were attributed to its interconnected microporous structure, which provided additional sites for Na-ion storage and enhanced the transport of sodium ions and electrons through the electrode.

The rate performance of MC3 is shown in Fig. 9(b). MC3 displays the reversible capacities of 370, 344, 321, and 279 mAh/g at 100, 200, 500, and 1000 mA/g, respectively. MC3 was adequately durable to withstand high current densities owing to its microporous structure. The KOH activation process creates micropores on hard carbon by etching effect, providing a high surface area of 808 m^2/g and large interlayer spacing in MC3. Enhanced Na-ion storage and shortening of ion transport pathways obtained due to the effect of its microporous structure can facilitate ion transport at high rates. Xu et al. [45] produced activated amorphous carbon from camellia pollen grains as an anode for SIBs via KOH activation of biomass followed by a two-step carbonization and acid etching process. It exhibited a good rate capability with reversible capacities of 324.8, 321.6, 312.1, 298.9, 282.3, and 272.4 mAh/g at 0.1, 0.2, 0.5, 1.0, 2.0, and 5.0 A/g, together with a surface area of 660.04 m^2/g. The results were ascribed to its high surface area with abundant micro- and mesopores and large interlayer spacing, which promotes fast ion transport, effective Na-ion intercalation, and adsorption.

Fig. 9(c) shows the high-rate cycling performance of MC3. MC3 exhibited a high initial specific capacity of 430 mAh/g. After two cycles, the specific capacity was decreased to around 280 mAh/g and the specific capacity was around 280 mAh/g at 1 A/g in 400 cycles. The great electrochemical performance of MC3 may be ascribed to its disordered microporous structure with a high surface area and a large interlayer spacing, which was achieved by HTC and KOH activation before pyrolysis. Wang et al. [46] fabricated microporous sulfur-doped carbon microtubes from cotton as anodes for SIBs via sulfurizing at 700 °C. They displayed a charge capacity of 281 mAh/g after 1000 cycles at 1 A/g with a surface area of 307.6 m^2/g. The results were attributed to its microporous structure, which provided additional sites for Na-ion storage and enhanced the transport of sodium ions and electrons through the electrode.

We presented an energy-efficient and effective method for producing waste cotton-based microporous carbon anodes for SIBs by low-temperature HTC, KOH activation, and pyrolysis without requiring pretreatment, mercerization, and purification. Moreover, the cellulose fibrillar structure of cotton enabled effective chemical activation, leading to improved pore development and increased surface area. Limited studies have been conducted on waste cotton-based carbon anodes for SIBs, and MC3 has demonstrated superior electrochemical performance along with a more energy-efficient synthesis method compared to previous studies, thanks to its microporous structure and high surface area of 808 m^2/g (Table 3). The meso-microporous structure promoted efficient and fast ion transport, while the abundance of pores reduced the diffusion distance for Na-ions, and numerous nanoscale pores could serve as reservoirs for Na-ion storage. The high surface area could ensure an extensive electrolyte-electrode interface for Na-ion adsorption and provide numerous active sites for charge-transfer reactions. The large interlayer spacing enhanced Na-ion transport and storage between graphene layers. Moreover, the porous structure could adapt to the

Table 3
Electrochemical characteristics of several cotton&cellulose-based carbons in sodium-ion batteries.

Material	Biomass precursor	Method	BET surface area, m^2/g	Specific capacity (mAh/g) at current density (A/g)	Electrolyte	Ref
Carbon film	Cotton cloth	Purification of cotton cloth and carbonization at 700 °C for 1 h	446.27	Around 200 at 0.01 for 250 cycles	1.0 M $NaSO_3CF_3$ in diglyme	[27]
Hard Carbon	Cotton fabric	Purification and cutting, and carbonization at 1000 °C for 1 h	70	240 at 0.05 after 100 cycles	NaFSI/C_3mpyrFSI electrolyte	[54]
Hard Carbon Microtubes	Cotton	One step direct pyrolysis at 1300 °C for 2 h	38	305 at 0.1 C after 100 cycles	A solution of 0.8 m $NaPF_6$ in ethylene and DMC (1:1 in volume)	[6]
Hard Carbon	Filter paper	Direct pyrolysis 800 °C for 2 h, grounding, washing in HCl, and KOH activation at 800 °C for 2 h	761	286 at 0.02 after 100 cycles	1 M solution of NaClO4 in a 1:1 vol/vol mixture of ethylene carbonate/propylene carbonate	[19]
PANi aerogel	Polyaniline (PANi), phytic acid	Oxidative polymerization of phytic acid, SiO_2 nanoparticles, and aniline, freeze drying, pyrolysis at 950 °C for 2 h, HF washing	1292.60	973 at 0.2 after 160 cycles	1 M $LiPF_6$ in a mixture of ethylene carbonate/diethyl carbonate (EC/DEC, 1:1 by volume)	[55]
Hard Carbon	Cotton snippets	Carbonization at 1200 °C for 5 min and then mixing with carbon black, carboxymethyl cellulose, and styrene-butadiene rubber	2	270 at 0.05 after 80 cycles	80 µL NaFSI/C_3mpyrFSI	[7]
Hard carbon	Cotton	Purification and pyrolysis at 1000 °C for 5 min	NA	272 at 0.05 after 100 cycles	80 µL NaFSI/C_3mpyrFSI	[4]
Flexible P-Doped Carbon	Cotton cloth	Calcination at 700 °C for 3 h, cutting and washing in HCl, and P-doping at 450 °C for 3 h and then 260 °C for 18 h	345.9	190 at 0.2 after 600 cycles	1 mol/L $NaClO_4$ in ethylene carbonate and propylene carbonate in a volume ratio of 1:1 with 5 % fluoroethylene carbonate	[56]
Hard Carbon	Cellulose	One step direct pyrolysis at 1300 °C for 1 h	7.12	373.2 at 0.03 after 200 cycles	1 M $NaClO_4$ in ethylene carbonate/ dimethyl carbonate (1:1 in volume)	[38]
Hard Carbon	Cellulose from wood	hydrolysis with sulfuric acid at 45 °C for 6 h and two-step carbonization at 240 °C (8 h) & 1000 °C (2 h)	145.56	300 at 0.1 over 400 cycles	1.0 M $NaClO_4$ in (1:1 V/V) ethylene carbonate/diethyl carbonate	[57]
Hard Carbon	Cellulose	Two step pyrolysis at 450 °C and 1600 °C for 1 h	below 10	About 230 at 0.0372 for 500 cycles	1 M solution of $NaPF_6$ in ethylene carbonate/dimethyl carbonate (1/1 in volume)	[58]
Hard Carbon	Waste Cotton	HTC at 250 °C for 4 h, KOH activation pyrolysis at 800 °C for 2 h	808	330 at 0.1 for 200 cycles	1 M $NaClO_4$ in ethylene carbonate propylene carbonate (v/v: 1/1)	This study

volume changes during the discharge-charge cycles.

Graphite is not a suitable anode material for SIBs and delivers a low sodium storage capacity of 31 mAh/g, due to the inefficient intercalation of Na-ions into graphite with the limited interlayer spacing (0.34 nm) [47]. In contrast, the MC3 provides a reversible capacity of 330 mAh/g, which is within the acceptable range for commercial applications. Today, commercial hard carbon anodes for SIBs have managed to reach a specific capacity of about 300 mAh/g [48]. Hence, the MC3 can be a viable and eco-friendly alternative to graphite for commercial SIB anodes. Liu et al. [49] studied market analysis for hard carbon anode materials, indicating that hard carbons have more potential to decrease production costs due to their broad range of precursor options in comparison with graphite. Moreover, hard carbons offer greater promise to lower the environmental burden and improved Na-ion storage performance than graphite [49]. KOH activation offers significant advantages, such as high surface areas and dominant microporosity. In addition, the KOH activation process has been improved to address some issues, including KOH recovery and wastewater treatment solutions. Montes et al. [50] studied the recycling of KOH from activated carbon, showing substantial amounts of KOH could be recovered by water-washing and acid-washing, and reused over multiple cycles. Kim and Lee [51] investigated three methods: acidification, ion exchange, and phase transition with $Ca(OH)_2$ to recover potassium compounds such as KOH during activation. Among them, phase transition is specified as a more economically viable recovery strategy, as it reduces costs by around 20 %. Moreover, it is regarded as a more favorable strategy, providing effective conversion of K_2CO_3 into KOH and forming reusable secondary byproducts for chemical activation relative to acidification and ion exchange methods.

The industrial applicability of biomass-derived hard carbon production is supported by the life-cycle assessment (LCA) and techno-economic analysis (TEA) studies in systems that are similar to our process. Li et al. [33] synthesized switchgrass-derived anode for SIBs by using HTC and carbonization (1600 °C for 2 h), and they performed LCA and TEA. Their results estimated the minimum carbon selling price for the production of hard carbons to be $1.72 per kg without wastewater treatment, and $1.58 per kg with the integration of wastewater treatment. This value is economically comparable to graphite and below the current hard carbon selling price. In addition, they reported that the HTC before carbonization decreases greenhouse gas emissions relative to conventional techniques [52]. Luanwuthi et al. [53] investigated the economic performance and environmental effect of oil palm leaves-derived activated carbon produced by applying feedstock pretreatment, HTC, and KOH activation. Their TEA showed that large-scale production (1080 tons/year) is economically feasible, achieving the highest profitability (17.458 million USD), and the lowest minimum selling price of $10.55 per kg, compared to small and medium-scale production. Their LCA indicated that KOH activation is the largest contributor to environmental effects such as freshwater toxicity and climate change. Thus, the study emphasized that incorporating KOH recovery and reuse into the system can reduce environmental impacts, and concluded that the activated carbon production by using HTC and chemical activation provides a significant economic advantage.

4. Conclusion

Waste cotton-based microporous carbon anodes for SIBs demonstrating superior electrochemical performance were fabricated using a sustainable source in a facile and cost-effective method. The waste cotton-based microporous carbons exhibited microporous structures with a large surface area due to the combination of HTC and KOH activation, followed by pyrolysis. Among the waste cotton-based microporous carbons, MC3 showed a high reversible capacity of 330 mAh/g at 0.1 A/g after 200 cycles, a high-rate capability, and a good cycling performance of 280 mAh/g at 1 A/g over 400 cycles. This outstanding performance of MC3 is based on the microporous structure with a surface area of 808 m^2/g and large interlayer spacing, which enables fast and efficient ion transport, allows the electrolyte to reach the active sites of the surface, and improves Na-ion storage. The method used in this work provides a novel approach to developing high-performance anodes for sustainable SIBs. However, the KOH activation causes environmental concerns for large-scale production because of the corrosive chemical usage and the formation of wastewater. To overcome these limitations, chemical recovery methods and wastewater treatment systems should be embedded within the process. Integration of these approaches is critical to reduce the environmental impacts of KOH activation and improve the viability and scalability of this method.

CRediT authorship contribution statement

Juran Kim: Writing – review & editing, Writing – original draft, Supervision, Conceptualization. **Murat Tosun:** Writing – review & editing, Writing – original draft, Project administration, Methodology, Conceptualization. **Ismail Topcu:** Writing – review & editing, Methodology, Investigation, Conceptualization. **Busra Temel:** Writing – original draft, Methodology, Investigation, Conceptualization. **Edip Bayram:** Writing – review & editing, Supervision, Methodology, Conceptualization. **Meltem Yanilmaz:** Writing – review & editing, Writing – original draft, Investigation, Funding acquisition, Formal analysis, Data curation, Conceptualization.

Funding Statement

This project has received funding from the European Union's Horizon 2020 Research and Innovation Programme under the Marie Skłodowska-Curie grant agreement No [101021759] and the Scientific Research Projects Department of Istanbul Technical University, ITU BAP (MGA-2023-43897). This research was also supported by the National Research Council of Science & Technology (NST) grant by the Korean government (MSIT) (No. CAP20022-000) and Korea Institute of Industrial Technology (PEO25030).

Declaration of Competing Interest

The authors declare that they have no known competing financial interests or personal relationships that could have appeared to influence the work reported in this paper.

Data availability

Data will be made available on request.

References

[1] F. Wang, T. Zhang, T. Zhang, T. He, F. Ran, Recent progress in improving rate performance of Cellulose-Derived carbon materials for Sodium-Ion batteries, Nano-Micro Lett. 16 (1) (2024) 148.
[2] M. Yan, Y. Qin, L. Wang, M. Song, D. Han, Q. Jin, S. Zhao, M. Zhao, Z. Li, X. Wang, Recent advances in biomass-derived carbon materials for sodium-ion energy storage devices, Nanomaterials 12 (6) (2022) 930.
[3] A. Al Rai, M. Yanilmaz, High-performance nanostructured bio-based carbon electrodes for energy storage applications, Cellulose 28 (9) (2021) 5169–5218.
[4] H.R. Sarma, J. Sun, Y. Hora, M. Forsyth, N. Byrne, Effect of carbonization behaviour of cotton biomass in electrodes for Sodium-Ion batteries, ChemElectroChem 10 (14) (2023) e202300127, https://doi.org/10.1002/celc.202300127.
[5] K.-l Hong, L. Qie, R. Zeng, Z.-q Yi, W. Zhang, D. Wang, W. Yin, C. Wu, Q.-j Fan, W.-x Zhang, Biomass derived hard carbon used as a high performance anode material for sodium ion batteries, J. Mater. Chem. A 2 (32) (2014) 12733–12738.
[6] Y. Li, Y.S. Hu, M.M. Titirici, L. Chen, X. Huang, Hard carbon microtubes made from renewable cotton as high-performance anode material for sodium-ion batteries, Adv. Energy Mater. 6 (18) (2016) 1600659.
[7] H.R. Sarma, J. Sun, I.E. Gunathilaka, Y. Hora, M. Forsyth, N. Byrne, Investigation of structural & interfacial properties of hard carbon electrodes from cotton snippets toward sustainable sodium-ion batteries, Sustain. Mater. Technol. 39 (2024) e00846.

[8] T.T. Ho, A. Nadeem, K. Choe, A review of upscaling hydrothermal carbonization, Energies 17 (2024).
[9] D. Alvira, D. Antorán, J.J. Manyà, Plant-derived hard carbon as anode for sodium-ion batteries: a comprehensive review to guide interdisciplinary research, Chem. Eng. J. 447 (2022) 137468.
[10] C. Hernández-Rentero, V. Marangon, M. Olivares-Marín, V. Gómez-Serrano, Á. Caballero, J. Morales, J. Hassoun, Alternative lithium-ion battery using biomass-derived carbons as environmentally sustainable anode, J. Colloid Interface Sci. 573 (2020) 396–408.
[11] Nagmani, P. Verma, S. Puravankara, Jute-fiber precursor-derived low-cost sustainable hard carbon with varying micro/mesoporosity and distinct storage mechanisms for sodium-ion and potassium-ion batteries, Langmuir 38 (50) (2022) 15703–15713.
[12] C. Falco, J.P. Marco-Lozar, D. Salinas-Torres, E. Morallón, D. Cazorla-Amorós, M. M. Titirici, D. Lozano-Castelló, Tailoring the porosity of chemically activated hydrothermal carbons: influence of the precursor and hydrothermal carbonization temperature, Carbon 62 (2013) 346–355, https://doi.org/10.1016/j.carbon.2013.06.017.
[13] J. Elisadiki, M.K. Gabookolwe, O.R. Onisuru, R. Meijboom, C. Muiva, C. K. King'ondu, Processing-properties-performance triad relationship in a washingtonia robusta mesoporous carbon materials-based supercapacitor device, RSC Adv. 12 (20) (2022) 12631–12646, 10.1039/D2RA01322C. DOI: 10.1039/D2RA01322C.
[14] J. González-Arias, M.E. Sánchez, J. Cara-Jiménez, F.M. Baena-Moreno, Z. Zhang, Hydrothermal carbonization of biomass and waste: a review, Environ. Chem. Lett. 20 (1) (2022) 211–221, https://doi.org/10.1007/s10311-021-01311-x.
[15] E. Canbaz, M. Aydin, R. DemIR-ÇAkan, Investigation of hazelnut shells driven hard carbons as anode for sodium-ion batteries produced by hydrothermal carbonization method, Turk. J. Chem. 46 (2022) 356–366.
[16] Z. Nie, Y. Huang, B. Ma, X. Qiu, N. Zhang, X. Xie, Z. Wu, Nitrogen-doped carbon with modulated surface chemistry and porous structure by a stepwise biomass activation process towards enhanced electrochemical lithium-ion storage, Sci. Rep. 9 (1) (2019) 15032.
[17] W. Chen, M. Gong, K. Li, M. Xia, Z. Chen, H. Xiao, Y. Fang, Y. Chen, H. Yang, H. Chen, Insight into KOH activation mechanism during biomass pyrolysis: chemical reactions between O-containing groups and KOH, Appl. Energy 278 (2020) 115730, https://doi.org/10.1016/j.apenergy.2020.115730.
[18] T. Sangprasert, V. Sattayarut, C. Rajrujithong, P. Khanchaitit, P. Khemthong, C. Chanthad, N. Grisdanurak, Making use of the inherent nitrogen content of spent coffee grounds to create nanostructured activated carbon for supercapacitor and lithium-ion battery applications, Diam. Relat. Mater. 127 (2022) 109164, https://doi.org/10.1016/j.diamond.2022.109164.
[19] P. Zheng, T. Liu, S. Guo, Micro-nano structure hard carbon as a high performance anode material for sodium-ion batteries, Sci. Rep. 6 (1) (2016) 35620.
[20] M. Wang, Z. Yang, W. Li, L. Gu, Y. Yu, Superior sodium storage in 3D interconnected nitrogen and oxygen dual-doped carbon network, Small 12 (19) (2016) 2559–2566.
[21] J. Xu, Q. Gao, Y. Zhang, Y. Tan, W. Tian, L. Zhu, L. Jiang, Preparing two-dimensional microporous carbon from pistachio nutshell with high areal capacitance as supercapacitor materials, Sci. Rep. 4 (1) (2014) 5545.
[22] M. Thommes, K. Kaneko, A.V. Neimark, J.P. Olivier, F. Rodriguez-Reinoso, J. Rouquerol, K.S.W. Sing, Physisorption of gases, with special reference to the evaluation of surface area and pore size distribution (IUPAC Technical Report), Pure Appl. Chem. 87 (9-10) (2015) 1051–1069, https://doi.org/10.1515/pac-2014-1117 (accessed 2024-09-28).
[23] S. Chaisit, N. Chanlek, J. Khajonrit, T. Sichumsaeng, S. Maensiri, Preparation, characterization, and electrochemical properties of KOH-activated carbon from cassava root, Mater. Res. Express 7 (10) (2020) 105605, https://doi.org/10.1088/2053-1591/abbf84.
[24] Y. Zhu, M. Chen, Q. Li, C. Yuan, C. Wang, A porous biomass-derived anode for high-performance sodium-ion batteries, Carbon 129 (2018) 695–701, https://doi.org/10.1016/j.carbon.2017.12.103.
[25] R. Nandi, M.K. Jha, S.K. Guchhait, D. Sutradhar, S. Yadav, Impact of KOH activation on rice husk derived porous activated carbon for carbon capture at flue gas alike temperatures with high CO2/N2 selectivity, ACS Omega 8 (5) (2023) 4802–4812, https://doi.org/10.1021/acsomega.2c06955.
[26] J. Xiang, W. Lv, C. Mu, J. Zhao, B. Wang, Activated hard carbon from Orange peel for lithium/sodium ion battery anode with long cycle life, J. Alloy. Compd. 701 (2017) 870–874, https://doi.org/10.1016/j.jallcom.2017.01.206.
[27] X. Zhang, Y. Wan, K. Yang, K. Song, L. Mi, G. Zheng, X. Feng, W. Chen, Cotton Cloth-Induced flexible hierarchical carbon film for Sodium-Ion batteries, ChemElectroChem 7 (9) (2020) 2136–2144, https://doi.org/10.1002/celc.202000407 (accessed 2024/09/28).
[28] D. Luo, P. Han, L. Shi, J. Huang, J. Yu, Y. Lin, J. Du, B. Yang, C. Li, C. Zhu, et al., Biomass-derived nitrogen/oxygen co-doped hierarchical porous carbon with a large specific surface area for ultrafast and long-life sodium-ion batteries, Appl. Surf. Sci. 462 (2018) 713–719, https://doi.org/10.1016/j.apsusc.2018.08.106.
[29] Y. Lv, F. Zhang, Y. Dou, Y. Zhai, J. Wang, H. Liu, Y. Xia, B. Tu, D. Zhao, A comprehensive study on KOH activation of ordered mesoporous carbons and their supercapacitor application, J. Mater. Chem. 22 (1) (2012) 93–99, https://doi.org/10.1039/C1JM12742J.
[30] F. Amran, M.A.A. Zaini, Effects of chemical activating agents on physical properties of activated carbons – a commentary, Water Pract. Technol. 15 (4) (2020) 863–876, https://doi.org/10.2166/wpt.2020.094 (accessed 6/18/2025).
[31] S. Guo, B. Guo, R. Ma, Y. Zhu, J. Wang, KOH activation of coal-derived microporous carbons for oxygen reduction and supercapacitors, RSC Adv. 10 (27) (2020) 15707–15714, https://doi.org/10.1039/D0RA01705A.
[32] A. Beda, C. Villevieille, P.-L. Taberna, P. Simon, C.M. Ghimbeu, Self-supported binder-free hard carbon electrodes for sodium-ion batteries: insights into their sodium storage mechanisms, J. Mater. Chem. A 8 (11) (2020) 5558–5571.
[33] Y. Li, D. Xia, L. Tao, Z. Xu, D. Yu, Q. Jin, F. Lin, H. Huang, Hydrothermally assisted conversion of switchgrass into hard carbon as anode materials for Sodium-Ion batteries, ACS Appl. Mater. Interfaces (2024).
[34] Z.-Q. Hao, J.-P. Cao, Y. Wu, X.-Y. Zhao, Q.-Q. Zhuang, X.-Y. Wang, X.-Y. Wei, Preparation of porous carbon sphere from waste sugar solution for electric double-layer capacitor, J. Power Sources 361 (2017) 249–258.
[35] A.A. Arie, H. Kristianto, E. Demir, R.D. Cakan, Activated porous carbons derived from the Indonesian Snake fruit peel as anode materials for sodium ion batteries, Mater. Chem. Phys. 217 (2018) 254–261, https://doi.org/10.1016/j.matchemphys.2018.06.076.
[36] H. Wang, W. Yu, J. Shi, N. Mao, S. Chen, W. Liu, Biomass derived hierarchical porous carbons as high-performance anodes for sodium-ion batteries, Electrochim. Acta 188 (2016) 103–110, https://doi.org/10.1016/j.electacta.2015.12.002.
[37] I. Jeon, T. Kim, J. Seo, I.-K. Jeong, J.H. Lee, M. Park, Y. Park, D. Yang, C.R. Cho, Enhanced electrochemical performance and interdiffusion behavior of sodium ions in onion-derived freeze-dried and KOH-activated carbon for sodium-ion battery anodes, Appl. Surf. Sci. 648 (2024) 159023, https://doi.org/10.1016/j.apsusc.2023.159023.
[38] L. Qin, S. Xu, Z. Lu, L. Wang, L. Chen, D. Zhang, J. Tian, T. Wei, J. Chen, C. Guo, Cellulose as a novel precursor to construct high-performance hard carbon anode toward enhanced sodium-ion batteries, Diam. Relat. Mater. 136 (2023) 110065, https://doi.org/10.1016/j.diamond.2023.110065.
[39] D. Antorán, D. Alvira, M.E. Peker, H. Malón, S. Irusta, V. Sebastián, J.J. Manyà, Waste hemp hurd as a sustainable precursor for affordable and High-Rate hard Carbon-Based anodes in Sodium-Ion batteries, Energy Fuels 37 (13) (2023) 9650–9661, https://doi.org/10.1021/acs.energyfuels.3c01040.
[40] J.J. Togonon, P.-C. Chiang, H.-J. Lin, W.-C. Tsai, H.-J. Yen, Pure Carbon-based electrodes for Metal-ion batteries, Carbon Trends 3 (2021) 100035, https://doi.org/10.1016/j.cartre.2021.100035.
[41] Y. Youn, B. Gao, A. Kamiyama, K. Kubota, S. Komaba, Y. Tateyama, Nanometer-size na cluster formation in micropore of hard carbon as origin of higher-capacity Na-ion battery, npj Comput. Mater. 7 (1) (2021) 48, https://doi.org/10.1038/s41524-021-00515-7.
[42] M. Yanilmaz, B. Temel, L. Chen, X. Zhang, High-performance cellulose-based nanostructured carbons for rechargeable batteries, J. Alloy. Compd. 1005 (2024) 175961.
[43] H. Wang, W. Yu, N. Mao, J. Shi, W. Liu, Effect of surface modification on high-surface-area carbon nanosheets anode in sodium ion battery, Microporous Mesoporous Mater. 227 (2016) 1–8, https://doi.org/10.1016/j.micromeso.2016.02.003.
[44] L. Cao, W. Hui, Z. Xu, J. Huang, P. Zheng, J. Li, Q. Sun, Rape seed shuck derived-lamellar hard carbon as anodes for sodium-ion batteries, J. Alloy. Compd. 695 (2017) 632–637, https://doi.org/10.1016/j.jallcom.2016.11.135.
[45] K. Xu, Y. Li, J. Xiong, X. Ou, W. Su, G. Zhong, C. Yang, Activated amorphous carbon with High-Porosity derived from camellia pollen grains as anode materials for Lithium/Sodium ion batteries, Front. Chem. 6 (2018), https://doi.org/10.3389/fchem.2018.00366.
[46] Q. Wang, X. Ge, J. Xu, Y. Du, X. Zhao, L. Si, X. Zhou, Fabrication of microporous sulfur-doped carbon microtubes for high-performance sodium-ion batteries, ACS Appl. Energy Mater. 1 (11) (2018) 6638–6645.
[47] Z. Zeng, Y. Mao, Z. Hu, K. Chen, Q. Huang, Y. Song, Z. Wu, P. Zhang, T. Chen, X. Guo, Research progress and commercialization of biologically derived hard carbon anode materials for Sodium-Ion batteries, Ind. Eng. Chem. Res. 62 (38) (2023) 15343–15359, https://doi.org/10.1021/acs.iecr.3c00818.
[48] B. Zhong, C. Liu, D. Xiong, J. Cai, J. Li, D. Li, Z. Cao, B. Song, W. Deng, H. Peng, et al., Biomass-Derived hard carbon for Sodium-Ion batteries: basic research and industrial application, ACS Nano 18 (26) (2024) 16468–16488, https://doi.org/10.1021/acsnano.4c03484.
[49] H. Liu, M. Baumann, X. Dou, J. Klemens, L. Schneider, A.-K. Wurba, M. Häringer, P. Scharfer, H. Ehrenberg, W. Schabel, et al., Tracing the technology development and trends of hard carbon anode materials - a market and patent analysis, J. Energy Storage 56 (2022) 105964, https://doi.org/10.1016/j.est.2022.105964.
[50] V. Montes, J.M. Hill, Activated carbon production: recycling KOH to minimize waste, Mater. Lett. 220 (2018) 238–240, https://doi.org/10.1016/j.matlet.2018.03.019.
[51] S. Kim, S.-E. Lee, Recovery of reactive potassium compounds as chemical agents in wastewaters from KOH-activated carbon production, Carbon Lett. (2025), https://doi.org/10.1007/s42823-025-00911-9.
[52] Li, Y.; Xu, Y.; Cheng, Y.; O'keefe, S.F.; Ogejo, J.A.; Lin, F.; Huang, H. Techno-Economic Analysis of Cost-Competitive Hard Carbon Production from Biomass for Sodium-Ion Batteries. 2025. DOI: http://dx.doi.org/10.2139/ssrn.5269420 (Accessed 28 Jun 2025).
[53] S. Luanwuthi, P. Iamprasertkun, T. Akkharaamnuay, C. Kunyawut, A. Phukhrongthung, C. Puchongkawarin, Techno-economic and environmental assessment of activated carbon electrodes for supercapacitors from oil palm leaves, ACS Sustain. Chem. Eng. 12 (39) (2024) 14446–14458, https://doi.org/10.1021/acssuschemeng.4c04783.
[54] H.R. Sarma, J. Sun, I.E. Gunathilaka, Y. Hora, R. Rajkhowa, M. Forsyth, N. Byrne, Effect of precursor morphology of cellulose-based hard carbon anodes for sodium-

ion batteries, Front. Batter. Electrochem. 2 (2024), https://doi.org/10.3389/fbael.2023.1330448.
[55] H. Liu, W. Zeng, Y. Yang, J. Chen, Y. Zhao, S. Mu, Synchronously improved graphitization and surface area in a 3D porous carbon network as a high capacity anode material for lithium/sodium-ion batteries, J. Mater. Chem. A 9 (2) (2021) 1260–1268, https://doi.org/10.1039/D0TA10179F.
[56] H.-Y. Lü, X.-H. Zhang, F. Wan, D.-S. Liu, C.-Y. Fan, H.-M. Xu, G. Wang, X.-L. Wu, Flexible P-Doped carbon cloth: Vacuum-Sealed preparation and enhanced Na-Storage properties as Binder-Free anode for sodium ion batteries, ACS Appl. Mater. Interfaces 9 (14) (2017) 12518–12527, https://doi.org/10.1021/acsami.7b01986.
[57] H. Zhu, F. Shen, W. Luo, S. Zhu, M. Zhao, B. Natarajan, J. Dai, L. Zhou, X. Ji, R. S. Yassar, et al., Low temperature carbonization of cellulose nanocrystals for high performance carbon anode of sodium-ion batteries, Nano Energy 33 (2017) 37–44, https://doi.org/10.1016/j.nanoen.2017.01.021.
[58] V. Simone, A. Boulineau, A. de Geyer, D. Rouchon, L. Simonin, S. Martinet, Hard carbon derived from cellulose as anode for sodium ion batteries: dependence of electrochemical properties on structure, J. Energy Chem. 25 (5) (2016) 761–768, https://doi.org/10.1016/j.jechem.2016.04.016.